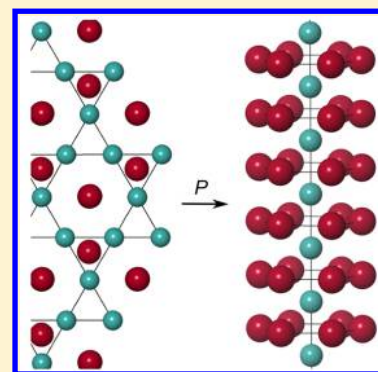


Enhanced Reactivity of Lithium and Copper at High Pressure

Jack Binns,[†] Philip Dalladay-Simpson,[†] Mengnan Wang,[†] Eugene Gregoryanz,^{†,‡} and Ross T. Howie^{*,†}[†]Center for High Pressure Science & Technology Advanced Research (HPSTAR), Shanghai 201203, People's Republic of China[‡]Centre for Science at Extreme Conditions and School of Physics and Astronomy, University of Edinburgh, Edinburgh EH9 3JZ, United Kingdom

ABSTRACT: High pressure can profoundly affect the electronic structure and reactivity, creating compounds between elements that do not react at ambient conditions. Lithium is known to react with gold and silver; however, no copper compounds are known to date. By compressing mixtures of the elements in diamond-anvil cells, compounds of lithium and copper have been synthesized and characterized by X-ray diffraction for the first time. Pressures as low as 1 GPa lead to the formation of a complex layered phase LiCu, displaying two-dimensional kagomé lattice layers of Cu atoms. With increasing pressure, the layered Cu–Cu bonding is replaced by linear chains of Cu atoms in the high-pressure phase Li₂Cu. Here we show the powerful effects of even modest pressures on the reactivity of lithium, leading to structures of remarkable complexity and low-dimensional transition metal bonding.



At atmospheric pressure, binary compounds of lithium (Li) and the noble metals gold (Au) and silver (Ag) have been known for some time. Exploration of the composition–temperature phase diagrams have revealed a wealth of different structures and compositions ranging from simple, cubic phases such as LiAg, Li₃Au, and LiAu₃ to highly complex “gamma-brass” structures in compounds such as Li₉Ag₄ and Li₁₅Au₄, which contain more than 75 atoms in the unit cell.^{1–4} Given the wealth of structural variety, it is perhaps surprising that Li and copper (Cu) are reportedly unreactive, forming no known compounds despite extensive investigation.^{5–8}

The use of high-pressure reaction conditions is a widely exploited technique to synthesize novel compounds with unusual physical and chemical properties.^{9–12} The reactivity of Li under pressure has attracted significant attention, but to date, studies have been limited to structure-searching algorithms and density functional theory. A number of Li compounds have been predicted to form at high pressures with Be,¹³ Au,¹⁴ Zn,¹⁵ and Fe,¹⁶ making this a promising approach to modulate the reactivity of the Li–Cu system. It should also be noted that because of the reported inertness, Cu has been widely used as an electrode for conductivity measurements of Li under pressure; however, the possibility of reaction between the two species has not been explored.^{17–19}

Here we show that the application of even modest pressures, i.e., <1 GPa (<10000 atm), causes the reaction of Li and Cu, forming previously unknown compounds at room temperature. The structures of these phases have been determined by high-pressure X-ray diffraction. At low pressures, we observe a complex phase, with stoichiometry LiCu, consisting of layers of Cu atoms arranged in a kagomé lattice. Above 5 GPa, the Cu–Cu bonding changes drastically: transitioning from 2D layers to linear chains of Cu atoms observed in the high-pressure Li₂Cu

phase. This phase is stable to 25 GPa, the highest pressure reached in this study.

During loading of the DACs, grains of Cu powder were placed directly on the surface of the Li metal with no visible reaction occurring. After sealing the sample in the DAC gasket chamber while in an inert atmosphere, the Cu powder lost its characteristic color, leaving gray, textured regions on the surface of the sample. Attempts were made to keep the initial pressure as low as possible while also maintaining a hermetic seal on the sample chamber; the lowest pressure achieved was 0.9(1) GPa. X-ray diffraction data at this pressure is shown in Figure 1 and is highly complex, containing peaks due to unreacted Cu and Li, indicating that the system did not fully reach equilibrium. However, all remaining peaks can be indexed to a rhombohedral unit cell, $a = 4.9304(3)$ Å, $c = 26.193(1)$ Å at 0.9 GPa. Diffraction patterns for this phase were typically highly “spotty”, leading to unreliable integrated intensities, although unit cell dimensions could be extracted. However, one run produced powder diffraction rings of sufficient quality to allow Rietveld full profile refinement. Solution of the structure reveals a new “ μ -phase” intermetallic with stoichiometry Li_{19.5}Cu_{19.5} (in Pearson notation: LiCu-R39). Two Cu atom sites were readily identified at the 18*h* and 3*a* sites, one fully ordered (18*h*) and one-half-occupied (3*a*). Three Li atom sites were located in difference Fourier maps; the fourth half-occupied site is shared with Cu (Figure 2).

The stoichiometry of this phase was determined by refining the occupancy of the disordered Cu atom site, and this is in agreement with volume vs pressure relationships for the LiCu-R39 phase compared to hypothetical volumes for Li–Cu alloys

Received: April 28, 2018

Accepted: May 22, 2018

Published: May 22, 2018

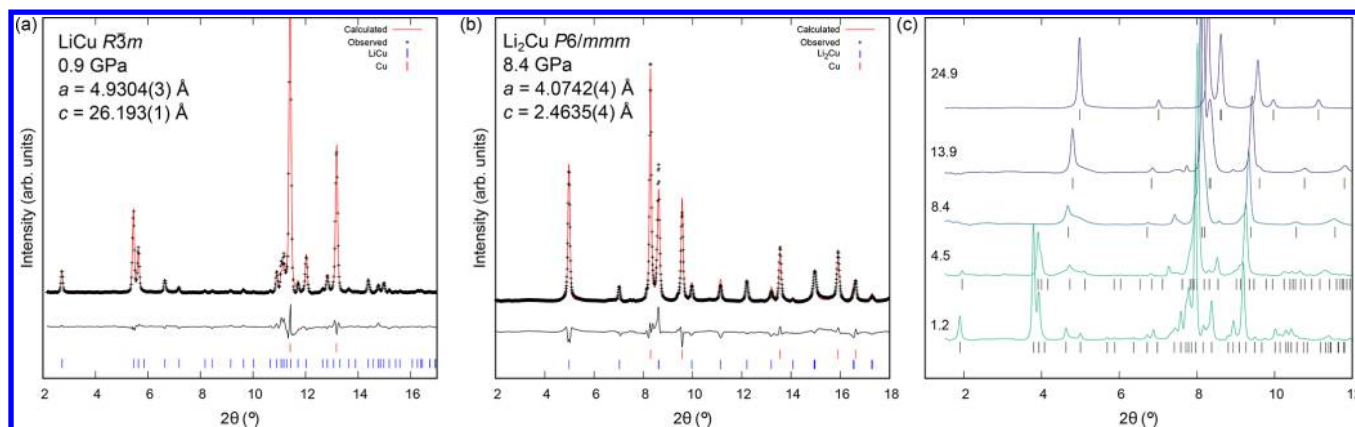


Figure 1. X-ray diffraction patterns collected at (a) 0.9 GPa ($\lambda = 0.4136 \text{ \AA}$) showing the numerous peaks corresponding to the low-pressure phase $\text{Li}_{19.5}\text{Cu}_{19.5}$. Tick marks indicate the location of Bragg peaks from $\text{Li}_{19.5}\text{Cu}_{19.5}$, and Cu. (b) X-ray diffraction pattern ($\lambda = 0.2889 \text{ \AA}$) collected at 24.9 GPa. All peaks can be indexed to a hexagonal high-pressure compound Li_2Cu crystallizing in $P6/mmm$, which remains stable to at least 24.9 GPa. (c) X-ray diffraction patterns ($\lambda = 0.2889 \text{ \AA}$) showing the transition from LiCu to Li_2Cu . Tick marks indicate peaks from Li–Cu compounds, unmarked peaks are due to Cu and Li, and pressures (GPa) are given in corresponding labels.

obeying Vegard's law with formula $\text{Li}_{19.5}\text{Cu}_{19.5}$ (see Figure 3a and inset). Due to the low scattering factor for Li, the Li atomic coordinates for this phase could not be stably refined; however, the locations as determined from Fourier difference maps are reported in Table 1 and are in general agreement with those found for analogous μ -phase structures. The final agreement factors for refinement against the data at 0.9 GPa are $wR_p = 0.022$ and $R_p = 0.013$ (Figure 1a).

μ -Phase intermetallics have been found in at least 12 binary A–B systems, where A and B are both transition metals, A from row 4 or 5 and B from row 3.^{20–24} These phases can show a range of stoichiometries with A varying between 40 and 55% depending upon the identities of A and B.²² To our knowledge, this is the first known example of a μ -phase intermetallic structure formed by an alkali metal.

LiCu has a layered structure; each unit cell contains six layers of Cu atoms arranged in two symmetry-independent kagomé lattices with Cu–Cu distances of 2.381(12) and 2.550(12) Å at 1.25 GPa. These Cu–Cu bonds are shorter than those in bulk Cu at the same pressure, reflecting the reduced dimensionality of the Cu–Cu bonding (Figure 3b). This strong Cu–Cu bonding results in highly anisotropic compressibility, with linear moduli for the two axes being 282(76) and 93(10) GPa for a and c , respectively.

LiCu-R39 is stable to 4.75 GPa, above which peaks corresponding to this phase began to disappear to be replaced by a smaller number of peaks corresponding to a new high-pressure phase and accompanied by a broad band of diffuse scattering centered on the (104) reflection (see Figure 1c). By 8.4 GPa, the transformation was complete. Again, X-ray diffraction patterns contained peaks corresponding to unreacted Cu and Li. The additional lines could be readily indexed to a hexagonal cell with unit cell dimensions (at 8.4 GPa) $a = 4.0742(4) \text{ \AA}$ and $c = 2.4635(4) \text{ \AA}$.

Structure solution by charge flipping²⁵ and subsequent Rietveld analysis shows the phase to have composition Li_2Cu and space group $P6/mmm$ (CaHg₂-type), analogous to Li_2Pt .²⁶ The final agreement factors for refinement against the data at 24.9 GPa are $wR_p = 0.015$ and $R_p = 0.007$ (Figure 1b). In this phase, Cu atoms (at (0, 0, 0) $1a$) are arranged in chains along the c -axis, and each chain passes perpendicular through stacks of Li atoms (at (1/3, 2/3, 1/2) $2d$) arranged hexagonally,

forming graphene-like sheets (Figure 2). Each Cu atom is coordinated by 12 Li atoms and 2 Cu atoms, forming stacked hexagonal prisms. Upon decompression, Li_2Cu remains stable to 4.6 GPa, below which peaks due to this phase disappear to be fully replaced by those of LiCu-R39 by 2.6 GPa.

A recent series of high-pressure experiments studying the electronic properties of Li up to 100 GPa utilized Cu electrodes to measure the resistivity of a Li sample.^{17–19} Our study shows that even at pressures created during loading we form Li–Cu compounds that persist to at least 25 GPa. Even though the resistivity studies were conducted at low temperatures, initial loadings were performed at room temperature; therefore, the samples would nevertheless contain significant contamination.

In LiCu-R39, there are three symmetry-independent Cu–Cu nearest-neighbor distances: two within the kagomé layers and one to the disordered Cu site between these layers. Under compression, Cu–Cu distances within one of the two layers increase (+0.12(2) Å) under pressure while reducing (–0.17(2) Å) in the other. Upon transition to Li_2Cu , Cu atoms form chains with only one nearest neighbor (distance give by unit cell length c), which is only marginally shorter than the interatomic distance in pure Cu at the same pressure, shown by the solid line in Figure 3b. The same holds true for interlayer distances in LiCu (next-nearest neighbors), which, despite the significant scatter in these values, clearly resolve to a single value upon transitioning to Li_2Cu , corresponding to the a unit cell length.

The observation of Cu–Cu bonding in both phases is in marked contrast to all Li–Au and Li–Ag compounds observed to date. Broadly, Li–Au and Li–Ag compounds are characterized by Au/AgLi_{*n*} polyhedra, with n ranging from 6 to 12, with variations in the exact arrangement of the units. The relationships between (negative) oxidation states and bonding within late transition metal compounds have been widely explored at ambient pressures,^{27,28} and this contrast can be understood in the differing electron affinities of Au and Cu.^{29,30} The high electron affinity of Au (222.747(3) kJ mol^{–1}) leads to formation of auride (Au^-) species with strong ionic character, making covalent Au–Au bonding unfavorable. By contrast, Cu has a lower electron affinity (119.235(4) kJ mol^{–1}), tending to favor the formation of low-dimensional covalent bonding.

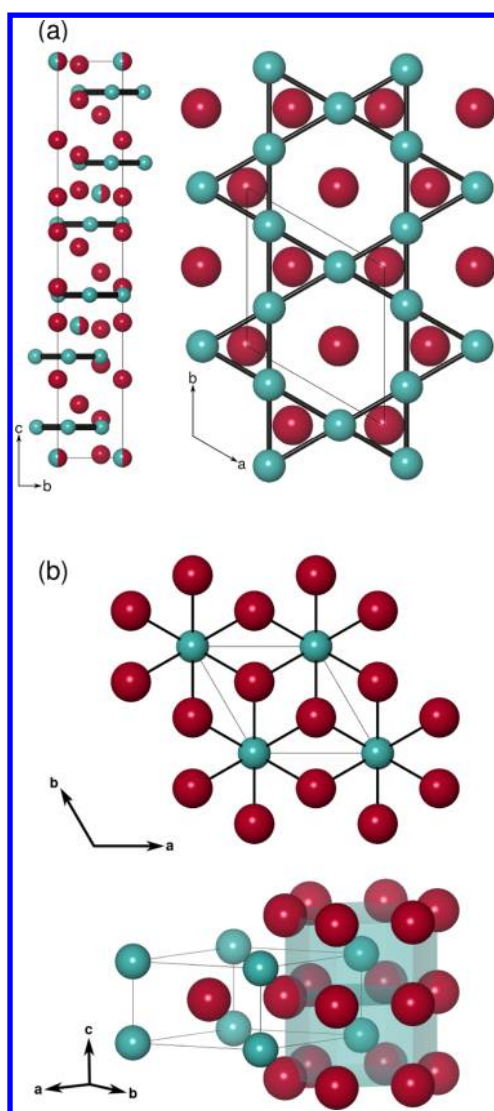


Figure 2. (a) Crystal structure of LiCu-R39 showing the copper kagomé lattices stacked along the c -axis. The right panel shows a single lattice layer. (b) The structure of Li_2Cu consists of Li_{12}Cu hexagonal prisms stacked along the c -axis. Lithium atoms are shown in red, and copper atoms are shown in blue.

The effect of this Cu–Cu transition metal bonding on the electronic structures of LiCu and Li_2Cu is an intriguing open question. For example, compounds adopting the $P6/mmm$ structure of Li_2Pt ²⁶ (among other CaHg_2 -type compounds) have been proposed to exhibit Dirac semimetal behavior as a result of linear chains of atoms ordered hexagonally in two dimensions.³¹ In calculations, spin–orbit coupling leads to the “gapping-out” of the Dirac semimetal state in Li_2Pt ; however, the strength of spin–orbit coupling is dependent on the atomic number of the atoms forming the chains and scales as Z^2 . The combination of weaker spin–orbit coupling and the large stable pressure range in which interatomic distances can be tuned (at least 20 GPa) makes Li_2Cu an intriguing candidate material for exploring this phenomenon.

In conclusion, the application of modest pressures, i.e., <1 GPa, leads to the formation of the first unambiguously characterized Li–Cu compounds. At low pressures, we observe the formation of LiCu-R39, adopting a remarkably complex layered structure with Cu atoms arranged in kagomé lattices.

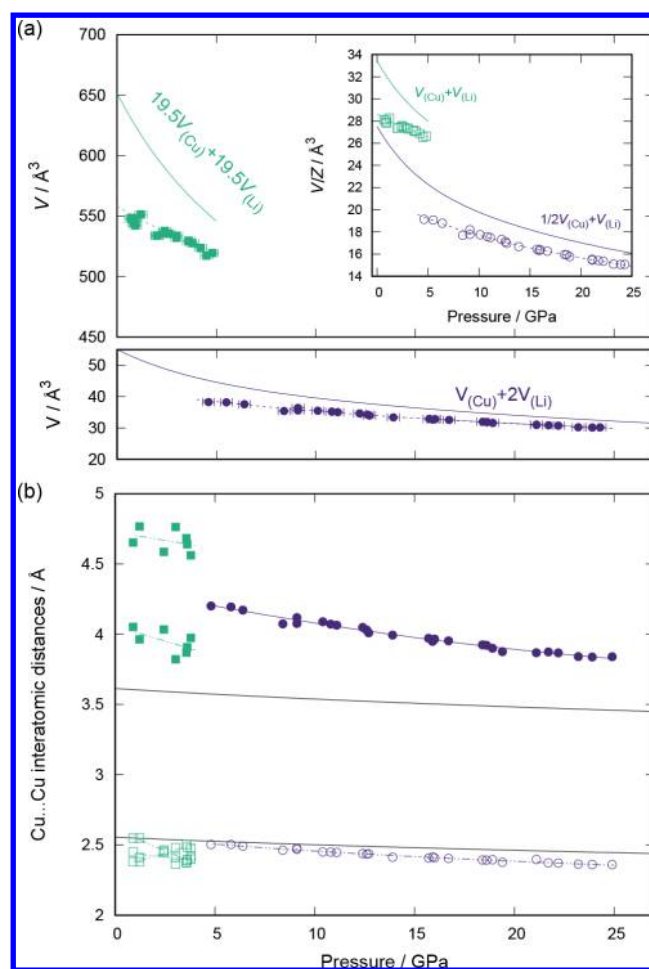


Figure 3. (a) Changes in unit cell volumes and volume-per-formula unit (V/Z) with pressure for Li–Cu compounds. Fitted equations-of-state are shown with dashed lines, and calculated volumes derived from atomic equations-of-state are shown with solid lines of corresponding color. (b) Changes in Cu...Cu interatomic distances with pressure for LiCu (green squares) and Li_2Cu (purple circles). Nearest-neighbor distances are shown with open symbols, and next-nearest-neighbor distances are shown with filled symbols. Corresponding distances in elemental Cu are shown with solid lines, and dashed lines are guides to the eye.

Table 1. Refined Atomic Position Parameters for LiCu-R39 at 0.9 GPa^a

atom	site	x	y	z
Cu1	18h	0.3240(10)	0.1620(5)	0.07758(11)
Cu2	3a	0	0	0
Li1	6c	2/3	1/3	0.13499
Li2	6c	1/3	2/3	0.09667
Li3	6c	1/3	2/3	0.00850
Li4	3a	0	0	0

^aParameters: $a = 4.9304(3)$ Å, $c = 26.193(1)$ Å, $V = 548.37(4)$ Å³, space group $R\bar{3}m$.

Above 5 GPa, LiCu-R39 is transformed to a new high-pressure phase Li_2Cu , which is stable to at least 25 GPa. This transition is marked by the reduction of Cu–Cu bonding from two-dimensional layers to one-dimensional chains. Our findings show the power of applying high pressure as an effective method for materials discovery.

All samples were made by the direct combination of Li and Cu loaded into diamond-anvil cells (DACs). All loadings were carried out in an argon atmosphere glovebox. Elemental Li (Alfa Aesar 99.9%) was first packed into the sample chamber formed by a rhenium gasket. Grains of Cu (Alfa Aesar 99.9%) were placed on the surface of the packed Li, and the cell was closed. The concentration of Cu was controlled by visual estimation during loading. Lithium presents a challenge for high-pressure experiments at room temperature as above pressures of 25 GPa Li reacts and diffuses into the diamond anvils, causing embrittlement and subsequent failure.³² As such, we limited our study to pressures below 25 GPa at room temperature.

Angle-dispersive X-ray diffraction patterns were recorded on PerkinElmer XRD21 and Marr345 image-plate detectors with synchrotron radiation sources with energies in the range of 30–42 keV. Two-dimensional image-plate data were integrated with DIOPRAS³³ to yield intensity vs 2θ plots. Patterns were indexed with GSAS-II,³⁴ and Le Bail³⁵ and Rietveld³⁶ refinements were carried out in JANA2006.³⁷

Pressure was determined with reference to the literature equation-of-state data for the elements Li³² and Cu.³⁸ Volume and linear equation-of-state parameters were determined using EOSFIT 7.³⁹

AUTHOR INFORMATION

Corresponding Author

*E-mail: ross.howie@hpstar.ac.cn.

ORCID

Jack Binns: 0000-0001-5421-6841

Notes

The authors declare no competing financial interest.

ACKNOWLEDGMENTS

The authors thank H. Maynard-Casely for helpful discussions. Parts of this research were carried out at P02.2 at DESY, a member of the Helmholtz Association (HGF). We would like to thank H.-P. Liermann and K. Glazyrin for assistance. Part of this work was performed under Proposal No. 2017A1062 at SPring-8. Portions of this work were performed at HPCAT (Sector 16), Advanced Photon Source (APS), Argonne National Laboratory. HPCAT operations are supported by DOE-NNSA under Award No. DE-NA0001974, with partial instrumentation funding by NSF. The Advanced Photon Source is a U.S. Department of Energy (DOE) Office of Science User Facility operated for the DOE Office of Science by Argonne National Laboratory under Contract No. DE-AC02-06CH11357. Funding has been provided by the respective Chinese “1000 Talent Award” grants of both P.D.S. and R.T.H.

REFERENCES

- (1) Freeth, W.; Raynor, G. The constitution of the system silver-lithium. *J. Inst. Met.* **1954**, *82*.
- (2) Kienast, G.; Verma, J.; Klemm, W. Das Verhalten der Alkalimetalle zu Kupfer, Silber und Gold. *Z. Anorg. Allg. Chem.* **1961**, *310*, 143–169.
- (3) Pavlyuk, V. V.; Dmytriv, G. S.; Tarasiuk, I. I.; Chumak, I. V.; Pauly, H.; Ehrenberg, H. Polymorphism of LiAg. *Solid State Sci.* **2010**, *12*, 274–280.
- (4) Noritake, T.; Aoki, M.; Towata, S.-i.; Takeuchi, T.; Mizutani, U. Structure determination of structurally complex Ag₃₆Li₆₄ gamma-brass. *Acta Crystallogr., Sect. B: Struct. Sci.* **2007**, *63*, 726–734.

- (5) Pastorello, S. Thermal analysis of the system lithium-copper. *Gazz. Chim. Ital.* **1930**, *60*, 988–992.
- (6) Klemm, W.; Volavšek, B. Zur kenntnis des systems lithium-kupfer. *Z. Anorg. Allg. Chem.* **1958**, *296*, 184–187.
- (7) Gasior, W.; Onderka, B.; Moser, Z.; Debski, A.; Gancarz, T. Thermodynamic evaluation of Cu-Li phase diagram from EMF measurements and DTA study. *CALPHAD: Comput. Coupling Phase Diagrams Thermochem.* **2009**, *33*, 215–220.
- (8) Van de Walle, A.; Moser, A.; Gasior, W. First-principles calculation of the Cu-Li phase diagram. *Arch. Metall. Mater.* **2004**, *49*, 535–544.
- (9) Grochala, W.; Hoffmann, R.; Feng, J.; Ashcroft, N. W. The chemical imagination at work in very tight places. *Angew. Chem., Int. Ed.* **2007**, *46*, 3620–3642.
- (10) Dewaele, A.; Worth, N.; Pickard, C. J.; Needs, R. J.; Pascarelli, S.; Mathon, O.; Mezouar, M.; Irifune, T. Synthesis and stability of xenon oxides Xe₂O₅ and Xe₃O₂ under pressure. *Nat. Chem.* **2016**, *8*, 784–790.
- (11) Howie, R. T.; Turnbull, R.; Binns, J.; Frost, M.; Dalladay-Simpson, P.; Gregoryanz, E. Formation of xenon-nitrogen compounds at high pressure. *Sci. Rep.* **2016**, *6*, 34896.
- (12) Hu, Q.; Kim, D. Y.; Yang, W.; Yang, L.; Meng, Y.; Zhang, L.; Mao, H.-K. FeO₂ and FeOOH under deep lower-mantle conditions and Earth's oxygen–hydrogen cycles. *Nature* **2016**, *534*, 241.
- (13) Feng, J.; Hennig, R. G.; Ashcroft, N. W.; Hoffmann, R. Emergent reduction of electronic state dimensionality in dense ordered Li-Be alloys. *Nature* **2008**, *451*, 445–448.
- (14) Yang, G.; Wang, Y.; Peng, F.; Bergara, A.; Ma, Y. Gold as a 6p-Element in Dense Lithium Aurides. *J. Am. Chem. Soc.* **2016**, *138*, 4046–4052.
- (15) Bi, H.; Zhang, S.; Wei, S.; Wang, J.; Zhou, D.; Li, Q.; Ma, Y. Globally stable structures of Li_xZn ($x = 1-4$) compounds at high pressures. *Phys. Chem. Chem. Phys.* **2016**, *18*, 4437–4443.
- (16) Zhou, Y.; Xu, Q.; Zhu, C.; Li, Q.; Liu, H.; Wang, H.; Tse, J. S. Predicted lithium-iron compounds under high pressure. *RSC Adv.* **2016**, *6*, 66721–66728.
- (17) Matsuoka, T.; Onoda, S.; Kaneshige, M.; Nakamoto, Y.; Shimizu, K.; Kagayama, T.; Ohishi, Y. Superconductivity and crystal structure of lithium under high pressure. *J. Phys. Conf. Ser.* **2008**, *121*, 052003.
- (18) Matsuoka, T.; Shimizu, K. Direct observation of a pressure-induced metal-to-semiconductor transition in lithium. *Nature* **2009**, *458*, 186–189.
- (19) Matsuoka, T.; Sakata, M.; Nakamoto, Y.; Takahama, K.; Ichimaru, K.; Mukai, K.; Ohta, K.; Hirao, N.; Ohishi, Y.; Shimizu, K. Pressure-induced reentrant metallic phase in lithium. *Phys. Rev. B: Condens. Matter Mater. Phys.* **2014**, *89*, 144103.
- (20) Kripyakevich, P.; Gladyshevskii, E.; Skolozdra, R. W₆Fe₇-type compounds in the Nb-Fe, Ta-Fe, and Ta-Co systems. *Sov. Phys., Cryst.* **1968**, *12*, 525–527.
- (21) Wagner, V.; Conrad, M.; Harbrecht, B. The μ -Phase of Co_{6.3}Nb_{6.7}. *Acta Crystallogr., Sect. C: Cryst. Struct. Commun.* **1995**, *51*, 1241–1243.
- (22) Joubert, J.; Dupin, N. Mixed site occupancies in the μ -phase. *Intermetallics* **2004**, *12*, 1373–1380.
- (23) Neal, B. P.; Ylvisaker, E. R.; Pickett, W. E. Quantum criticality in NbFe₂ induced by zero carrier velocity. *Phys. Rev. B: Condens. Matter Mater. Phys.* **2011**, *84*, 1–7.
- (24) Wang, J.; Feng, Y.; Jaramillo, R.; Van Wezel, J.; Canfield, P. C.; Rosenbaum, T. F. Pressure tuning of competing magnetic interactions in intermetallic CeFe₂. *Phys. Rev. B: Condens. Matter Mater. Phys.* **2012**, *86*, 1–7.
- (25) Oszlányi, G.; Süto, A. Ab initio structure solution by charge flipping. *Acta Crystallogr., Sect. A: Found. Crystallogr.* **2004**, *60*, 134–141.
- (26) Bronger, W.; Nacken, B.; Ploog, K. Zur synthese und struktur von Li₂Pt und LiPt. *J. Less-Common Met.* **1975**, *43*, 143–146.
- (27) Köhler, J.; Whangbo, M. H. Late transition metal anions acting as p-metal elements. *Solid State Sci.* **2008**, *10*, 444–449.

- (28) Lee, C.; Whangbo, M. H.; Kohler, J. Analysis of electronic structures and chemical bonding of metal-rich compounds. I. Density functional study of Pt Metal, LiPt₂, LiPt, and Li₂Pt. *J. Comput. Chem.* **2008**, *29*, 2154–2160.
- (29) Hotop, H.; Lineberger, W. C. Binding Energies in Atomic Negative Ions: III. *J. Phys. Chem. Ref. Data* **1985**, *14*, 731–750.
- (30) Bilodeau, R. C.; Scheer, M.; Haugen, H. K. Infrared laser photodetachment of transition metal negative ions: studies on Cr⁻, Mo⁻, Cu⁻, and Ag⁻. *J. Phys. B: At, Mol. Opt. Phys.* **1998**, *31*, 3885–3891.
- (31) Gibson, Q.; Schoop, L.; Muechler, L.; Xie, L.; Hirschberger, M.; Ong, N.; Car, R.; Cava, R. Three-dimensional Dirac semimetals: Design principles and predictions of new materials. *Phys. Rev. B: Condens. Matter Mater. Phys.* **2015**, *91*, 205128.
- (32) Guillaume, C. L.; Gregoryanz, E.; Degtyareva, O.; McMahon, M. I.; Hanfland, M.; Evans, S.; Guthrie, M.; Sinogeikin, S. V.; Mao, H.-K. Cold melting and solid structures of dense lithium. *Nat. Phys.* **2011**, *7*, 211–214.
- (33) Prescher, C.; Prakapenka, V. B. DIOPTAS: a program for reduction of two-dimensional X-ray diffraction data and data exploration. *High Pressure Res.* **2015**, *35*, 223–230.
- (34) Toby, B. H.; Von Dreele, R. B. GSAS-II: The genesis of a modern open-source all purpose crystallography software package. *J. Appl. Crystallogr.* **2013**, *46*, 544–549.
- (35) Le Bail, A.; Duroy, H.; Fourquet, J. Ab-initio structure determination of LiSbWO₆ by X-ray powder diffraction. *Mater. Res. Bull.* **1988**, *23*, 447–452.
- (36) Rietveld, H. M. A profile refinement method for nuclear and magnetic structures. *J. Appl. Crystallogr.* **1969**, *2*, 65–71.
- (37) Petříček, V.; Dušek, M.; Palatinus, L. Crystallographic computing system JANA2006: general features. *Z. Kristallogr. - Cryst. Mater.* **2014**, *229*, 345–352.
- (38) Dewaele, A.; Loubeyre, P.; Mezouar, M. Equations of state of six metals above 94 GPa. *Phys. Rev. B: Condens. Matter Mater. Phys.* **2004**, *70*, 1–8.
- (39) Gonzalez-Platas, J.; Alvaro, M.; Nestola, F.; Angel, R. EosFit7-GUI: a new graphical user interface for equation of state calculations, analyses and teaching. *J. Appl. Crystallogr.* **2016**, *49*, 1377–1382.